Construction and Building Materials 231 (2020) 117132

Contents lists available at ScienceDirect

Construction and Building Materials

journal homepage: www.elsevier.com/locate/conbuildmat

Self-sensing capability of Engineered Cementitious Composites: Effects of aging and loading conditions

Gürkan Yıldırım [a,*], Oğuzhan Öztürk [b], Ali Al-Dahawi [c], Adem Afşın Ulu [d], Mustafa Şahmaran [e]

[a] Department of Civil Engineering, Kırıkkale University, Kırıkkale, Turkey
[b] Department of Civil Engineering, Konya Technical University, Konya, Turkey
[c] Department of Civil Engineering, University of Technology, Baghdad, Iraq
[d] Department of Civil Engineering, Gazi University, Ankara, Turkey
[e] Department of Civil Engineering, Hacettepe University, Ankara, Turkey

HIGHLIGHTS

- Self-sensing capability of ECC with different carbon-based materials was assessed.
- Carbon fibers (CF), carbon nanotubes (CNT) and carbon black (CB) were used.
- Specimens cured for 7, 28, 90 and 180 days were used for self-sensing assessment.
- Tests were performed under compression, splitting tension and four-point bending.
- Self-sensing is valid for all curing ages and under different loading conditions.

ARTICLE INFO

Article history:
Received 8 July 2019
Received in revised form 9 September 2019
Accepted 1 October 2019
Available online 16 October 2019

Keywords:
Engineered Cementitious Composites (ECC)
Self-sensing
Curing age
Carbon fiber
Carbon nanotube
Carbon black

ABSTRACT

Self-sensing capability of 7-, 28-, 90- and 180-day-old Engineered Cementitious Composites (ECC) incorporated either with carbon fibers (CF/ECC-CF) at micro-scale or multi-walled carbon nanotubes (CNT/ECC-CNT) and carbon black (CB/ECC-CB) at nano-scale were investigated herein. Mechanical properties (compressive strength, splitting tensile strength/deformation, flexural strength/deformation) of different-age mixtures were evaluated. Control mixture (ECC-Control) without any carbon-based material was also produced and tested for comparison. Depending on the loading condition, equipment utilizing either direct current (DC) or alternating current (AC) was used for self-sensing assessments. Results showed that carbon-based materials generally improve the mechanical properties of ECC-Control specimens depending on the type of carbon-based materials, specimens' age and loading conditions. All specimens sensed different types of damage except 180-day-old ECC-Control specimens loaded under uniaxial compression and splitting tension due to abrupt increments in impedance results exceeding the limits of testing device which revealed the importance of presence of electrically-conductive materials for achieving enhanced self-sensing capability independent of aging, testing configuration/equipment, loading conditions and microcrack characteristics. CF is the best to improve self-sensing capability of ECC-Control specimens for all ages and loading conditions. Self-sensing performances of ECC-CNT and ECC-CB are comparable and utilization of nano-size carbon-based materials is suggested in cases where reversibility in self-sensing is needed.

1. Introduction

Structural design and environmental exposure conditions affect the durability and, relatedly, the serviceability of civil infrastructure. However, durability of concrete material is also very important and plays a vital role. Different from laboratory conditions, under service, structural concrete is subjected to different types of loads. Whatever the reason, concrete may crack as a result of loading. Despite the common understanding which state that cracking is anticipated and concrete structures are designed to crack, in reality, formation of cracks significantly fastens the deterioration and reduces the service life [1–3]. It is therefore very appealing for infrastructural longevity to lower the chances of cracking formation for concrete material.

* Corresponding author.
E-mail address: gyildirim@kku.edu.tr (G. Yıldırım).

https://doi.org/10.1016/j.conbuildmat.2019.117132
0950-0618/

Engineered cementitious composite (ECC) is a novel construction material capable of significantly delaying the onset and further propagation of cracking [4]. ECC is also known as strain-hardening cementitious composite (SHCC) in the open literature. As the name implies, the material is characterized with distinctive tensile stress-strain response which is realized through strain-hardening capability and coupled with the creation of many multiple tight microcracks under excessive tension-based loading scenarios [5–8]. Keeping the widths of cracks to minimum is one of the effective ways to prolong the serviceability of reinforced concrete structures which serve under harsh environmental exposures [1,9]. Accordingly, ECC, thanks to its multiple microcracking behavior, is constantly reported to stay durable under a wide range of severe environmental exposure conditions which trigger common durability problems (e.g. steel corrosion [2], sulfate attack [10], freeze/thaw effect [3,11] and alkali-silicate reaction [12]) for reinforced concrete structures. Improved durability of ECC materials under very harsh environmental exposures, even when severely damaged (i.e. microcracked), is not only related to the improved damage bearing capability but also autogenous self-healing capability which significantly reduces the transport of harmful agents into the materials [13–20].

On top of the superior mechanical, durability, self-healing properties, ECC is also reported to be inherently responsive to damage occurrence and this responsiveness is generally termed as the capability of "self-sensing". In general, self-sensing capability takes advantage of the dependence of electrical resistivity of concrete material on the damage created and can be quite rewarding to monitor the structural health, prevent the risks of sudden failure and increase the service life [21]. One can consider conventional ECC almost insulative and non-responsive to damage occurrence given the fact that individual constituents of the material are not conductive and mixing water diminishes with time due to progress in the hydration and pozzolanic reactions. However, literature clearly states that significantly high damage tolerance and excessive plastic deformation capability of ECC allow closer and more rigorous monitoring of damage through the changes in electrical measurements [22,23]. Moreover, as opposed to majority of self-sensing studies which concentrate on sensing of damage in compression (due to high brittleness of conventional concrete), ECC allows sensing of both compressive and tension-based damage [24].

On the other hand, electrical properties and hence, the self-sensing capability of cement-based materials can be significantly influenced by the changes in certain parameters such as the availability of water, chemistry and ionic condition of pore solution and ongoing hydration/pozzolanic reactions. For proper observation of the introduced damage, large variations in the electrical properties are undesirable. In order to reduce these variations and make sure higher consistency in the electrical measurements, it is a common practice to incorporate electrically-conductive materials into the cement-based systems including ECC [25,26]. However, even when incorporated with such materials, one can expect the interruption of electrically-conductive network of cementitious systems with the newly-produced hydration/pozzolanic reaction products either covering the electrically-conductive materials or directly blocking the path by densening of the microstructure [27]. As it is well-known, progress in the hydration/pozzolanic reactions is highly dependent on the aging. In order to maintain the effectiveness of self-sensing in ECC systems, it is therefore critical to ensure that the electrical properties, even when the material is aged, would stay the same and/or at acceptable levels to monitor the occurrence of damage.

In this study, self-sensing capability of ECC mixtures produced with different electrically-conductive carbon-based materials at micro- (carbon fibers [CF]) and nano-scale (multi-walled carbon nanotubes [CNT] and carbon black [CB]) was evaluated at the end of initial curing ages of 7, 28, 90 and 180 days to observe the effectiveness and extent of self-sensing capability. Special attention was also paid to the assessment of self-sensing capability under different loading scenarios. This is considered very important since almost all studies available in the literature tested the self-sensing capability of ECC under uniaxial tensile loading conditions [24,28–34]. Along these lines, self-sensing assessments were made under uniaxial compression, splitting tension and four-point bending loading. While recording and discussing the self-sensing results, effects of addition of different carbon-based materials on the mechanical properties of ECC mixtures under abovementioned loading conditions were also discussed.

2. Experimental program

2.1. Materials, mixing, mixture proportioning and specimen preparation

Raw materials used in the production of ECC mixtures were CEM I 42.5R ordinary Portland cement (PC), Class-F fly ash (FA) and fine silica sand with a maximum aggregate size of 0.4 mm, polyvinyl-alcohol (PVA) fibers, drinkable water and polycarboxylic ether-based high-range water reducer (HRWR). Chemical composition and physical properties of PC, FA and silica sand are given in Table 1. PVA fibers had length, diameter, specific gravity, nominal tensile strength and elastic modulus of 8 mm, 39 μm, 1.3, 1620 MPa and 42.8 GPa, respectively and they were used by 2% of total mixtures' volume (26 kg/m^3). ECC mixtures were produced with constant fly ash to Portland cement ratio (FA/PC) of 1.2, sand to Portland cement ratio of 0.36 and water to cementitious materials (FA + PC) ratio (W/CM) of 0.27.

Carbon-based electrically-conductive materials employed to create an electrical network within the cementitious composites were carbon fibers (CF), multi-walled carbon nanotubes (CNT) and carbon black (CB). Among these, only the CF was at micro-scale while the rest were at nano-scale. The length, diameter, aspect ratio, elongation, tensile strength, elastic modulus and density of CF were 12 mm, 7.5 μm, 1600, 1.8%, 4200 MPa, 240 GPa and 1.7 g/cm^3, respectively. CNT was 20–30 nm in diameter, 10–30 μm in length and had a surface area of more than 200 m^2/g. The surface area and average particle size of CB were around 30–50 m^2/g and 20–100 nm, respectively. SEM micrograph images of carbon-based materials used in the study are shown in Fig. 1.

Taking the overall cost of manufacture and agglomeration problems of different carbon-based materials into account (especially those that are at nano-scale), it is desirable to decide their utilization rates in compact ECC compositions rigorously. To account for this, a detailed study was performed by Al-Dahawi et al. [26] where the optimum utilization rates of abovementioned carbon-based materials were decided for 1-, 7-, 28-, 60-, 90- and 180-day-old ECC matrices to reach nearly the lowest electrical resistivity (highest electrical conductivity) results. These rates which were stated to be the electrical percolation thresholds were found to be 0.55% and 2.00% of the total weight of cementitious materials for CNT and CB, respectively while 1.00% of the total volume of mixtures for CF at the end of all predetermined testing ages. Since matrices with similar ages and ingredients were also used in this study, percolation thresholds reported for different carbon-based materials in [26] were also utilized in this study. ECC mixture denominations and proportions are shown in Table 2. As can be seen from this table that each individual mixture was denominated to give an idea about the carbon-based material it incorporates. In addition to ECC mixtures produced with different carbon-based materials, ECC-Control mixture which was plain and did not incorporate any carbon-based material was also produced for comparison.

Due to considerably different characteristics of carbon-based materials used in the production of mixtures, it was not an easy task to use similar HRWR contents for all mixtures. Therefore, instead of setting a constant HRWR content, similar workabilities (i.e. flow characteristics) were obtained for all ECC mixtures. Assurance of similar workabilities for different mixtures was made by performing a series of mini-slump flow tests. Based on these tests, HRWR contents for different mixtures were changed until reaching similar flow deformation levels with flow diameter of nearly 16 cm for all ECC mixtures. Details regarding the mini-slump tests performed on ECC mixtures with different carbon-based materials can be found in [25].

As the carbon-based materials used herein (especially those that are at nano-scale) are significantly small in size, they are very likely to face the problems of non-uniform dispersion and agglomeration. In a recent study undertaken by the authors [25], this issue was addressed in detail by proposing different mixing methods for carbon-based materials both at nano- and micro-scale. Accordingly, to uniformly distribute the carbon-based materials in ECC compositions, mixing methods individually suggested in [25] for nano- and micro-scale carbon-based materials were used for distributing CNT and CB, and CF, respectively. Since the details of proposed mixing methods were discussed in very much detail elsewhere [25], no further discussions were made here.

Table 1
Chemical composition and physical properties of PC, FA, silica sand.

Constituents	Chemical composition, %								Physical properties	
	SiO_2	Al_2O_3	Fe_2O_3	MgO	CaO	Na_2O	K_2O	Loss on ignition	Specific gravity (unitless)	Blaine fineness (m^2/kg)
PC	20.8	5.55	3.35	2.49	61.4	0.19	0.77	2.20	3.06	325
FA	52.2	16.6	6.60	2.10	7.98	0.86	1.53	10.4	2.10	269
Sand	99.8	0.06	0.02	0.01	0.02	0.02	0.01	0.07	2.60	–

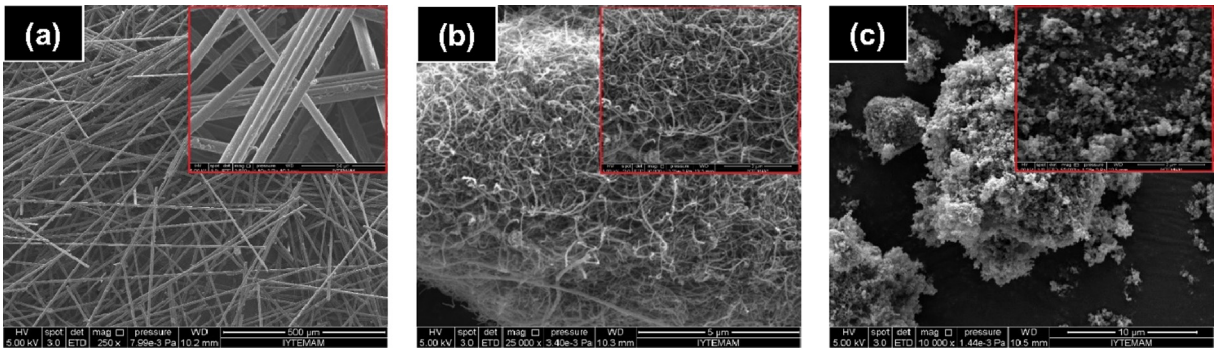

Fig. 1. SEM micrograph images of (a) CF, (b) CNT, (c) CB.

Table 2
Mixture proportions of different ECC mixtures relative to the mass of PC.

Mixture ID.	PC	Sand/PC	FA/PC	W/CM	PVA, kg/m^3	HRWR, kg/m^3	Carbon-based material, %
ECC-Control	1	0.36	1.2	0.27	26	4.5	–
ECC-CF	1	0.36	1.2	0.27	26	9.0	1.00*
ECC-CNT	1	0.36	1.2	0.27	26	17.0	0.55**
ECC-CB	1	0.36	1.2	0.27	26	15.0	2.00**

* : CF, by the total volume of mixture.
** : CNT and CB, by the total weight of cementitious materials (PC + FA).

Once the mixing methods of different carbon-based materials were decided, specimens for different loading conditions were started to be produced. For self-sensing assessment under compressive and splitting tensile loading, cubic specimens with the dimensions of 50 mm were produced while for the case of four-point bending loading, prismatic specimens with the dimensions of 360 × 75 × 50 mm were produced. To account for the possible variations in the results, from each mixture, three separate specimens were produced for each predetermined initial curing age (7, 28, 90 and 180 days). During the production of specimens, as the first step, fresh mixtures were poured into the oiled molds and kept there for 24 h at 50 ± 5% RH, 23 ± 2 °C with their surfaces covered with plastic sheets. After 24 h, specimens were demolded and put inside the isolated plastic bags for further curing at 95 ± 5% RH, 23 ± 2 °C until reaching 6, 27, 89 and 179 days of ages. Before self-sensing tests, after different curing periods, all specimens were moved into an oven set at 60 °C and kept there for 24 h for any misleading results that may arise due to the presence of excessive moisture. This dry conditioning method was previously applied by several researchers in the literature including the authors [26,35]. After the process of drying, all the tests were performed at room temperature. Loading rates during the compressive, splitting tensile and four-point bending loading cases were 0.36 MPa/s, 0.02 MPa/s and 0.005 mm/s, respectively. In addition to the self-sensing performance, basic mechanical properties of ECC mixtures under different loading conditions were determined and discussed in relation to the self-sensing capability.

2.2. Testing for self-sensing

Before the start of actual tests, preliminary works were performed to decide the configurations for proper measurement of electrical properties of specimens having different dimensions and subjected to different loading conditions. Self-sensing performance was assessed with the help electrical resistivity (ER) measurements recorded directly from specimens by using equipment which either employed alternating current (AC) technique with two probes or direct current (DC) technique with four probes. Different types of electrodes including steel/copper mesh and wire, brass plate, aluminum foil and conductive tapes were tried for properly recording the ER data. Taking the cost of manufacture, easy embeddability and sensitivity/accuracy of the ER results into account during the preliminary works, brass electrodes were decided to be used in the assessment of self-sensing performance [26,36].

Brass electrodes were benefited after they were embedded inside the specimens at fresh state. Brass electrodes of different sizes, numbers and embedment places together with measurements recorded with different equipment were also tried during the decision making of ER configurations under different loading conditions. Selection of the configurations shown in Fig. 2 was based on the ER results obtained with better sensitivity and accuracy under all loading conditions. The tests were performed with great care and electrical contacts were interrupted with the help of insulating covers each time of measurement for sensitivity.

2.2.1. Configuration for uniaxial compression and splitting tensile loading conditions

To evaluate self-sensing capability under uniaxial compression and splitting tensile loading, a configuration previously verified for uniaxial compression loading condition was used [26] (Fig. 2-a and b). In this configuration, brass electrodes which measure 10 mm in width and 60 mm in length were placed parallelly inside 50 mm-cubic specimens and measurements were recorded with the help of the 2-probe resistivity meter. Embedment places of the electrodes were very close to the top surface of cubic specimens and 5 mm inward from opposite sides. The only difference between compressive and splitting tensile loading conditions was that for splitting tensile loading, rebar with a square cross-section of 100 mm^2 was placed between the loading plates and specimen. 2-probe AC concrete resistivity meter used in self-sensing evaluation under compression and splitting tension was operated at a frequency of 1 kHz to intercept the polarization of current, as suggested by [26,37]. 2-probe AC resistivity meter gave impedance and corresponding phase angle results (ranged between 0°-180°) directly. These values were then used to obtain final ER results of specimens with the help of geometrical factors. Following equation was used for the calculations:

$$\rho = Z \times \cos(\theta) \times \frac{A}{L} \quad (1)$$

where, ρ, Z, θ, A and L stand for electrical resistivity (ER) (Ω.m), electrical impedance (Ω), phase angle (°), cross-sectional area (m^2) and length (m) of the specimen, respectively.

Fig. 2. Proposed configurations for ER measurements under (a) uniaxial compression (b) splitting tensile and (c) four-point bending loading.

2.2.2. Configuration for four-point bending loading condition

For self-sensing assessments under four-point bending loading, a configuration with previously validated performance was used (Fig. 2-c) [36]. In this configuration, four 10 × 100 (width × length) brass electrodes (two at each side) were placed parallelly in the tensile region of prismatic specimens. Electrodes were placed 25 mm away from the edges of the specimens (near support points) to prevent the localization of microcracks from region right under the upper loading feet which may lead to premature failure of specimens. Electrical measurements were made with the help of the 4-probe DC source meter. This device which was arranged to obtain the voltage and current simultaneously recorded the voltage data from the inner electrodes and used the outer electrodes to apply electrical current (Fig. 2-c). Ohm's law was applied by considering geometrical factors to determine the final resistivity values according to the equation given below:

$$\rho = \frac{V}{I} \times \frac{A}{L} \tag{2}$$

where, ρ, V, I, A and L stand for resistivity (Ω.m), measured voltage (mV), applied current (mA), cross-sectional area of the contact area between brass electrode and specimen (m^2), and distance (m) between the internal electrodes, respectively.

After evaluating the raw electrical resistivity results either by using the equipment utilizing AC or DC technique, the fractional changes in electrical resistivity (FCER, %) were calculated in accordance with the equation given below to represent the self-sensing behavior of ECC mixtures.

$$FCER\left(\frac{\Delta\rho}{\rho_o}\right)(\%) = \left(\frac{\rho_L - \rho_o}{\rho_o}\right)100 \tag{3}$$

where, ρ_L and ρ_o are the electrical resistivities during loading and initial electrical resistivity of tested specimens, respectively. Recorded FCER results were then drawn with respect to deformation results acquired under different loading conditions.

3. Results and discussion

3.1. Mechanical behavior under uniaxial compressive loading

In Fig. 3, average compressive strength results of ECC mixtures were shown for initial curing ages. Clearly, compressive strength results of all mixtures increased continuously with the extension

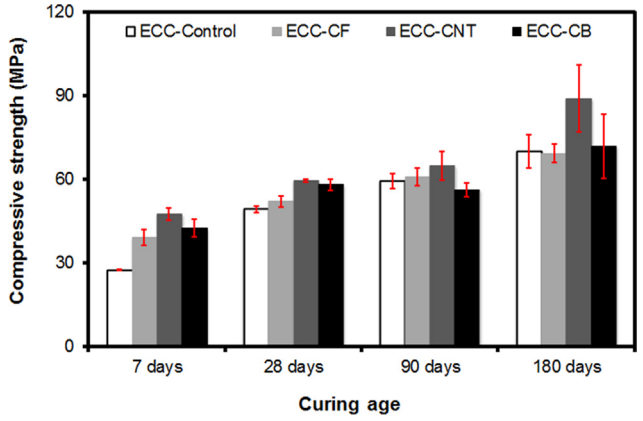

Fig. 3. Average compressive strength results of different-age ECC mixtures. Error bars are according to standard deviations.

of curing periods. This was expected due to advancements in the strength-developing reactions with time which resulted in less overall porosity and highly tortuos pore system, continuously increasing compressive strength results. However, the rates of strength increments with time were significantly different. For example, between the ages of 7 and 180 days, the average compressive strength results of ECC-Control, ECC-CF, ECC-CNT and ECC-CB mixtures increased by 155%, 77%, 87% and 72%, respectively. Lower rates of improvement in the compressive strength results of ECC mixtures with different carbon-based materials can be attributed to the significantly dense matrices of the specimens which got even denser with the incorporation of carbon-based materials (especially those at nano-scale [CNT and CB]) due to significantly larger specific surface areas of these materials. Upon further densening of the matrices, delays in the pozzolanic capacity and filler effect [38] and decrements in the available space for the settlement of products of hydration and pozzolanic reactions [26] are anticipated, all of which reducing the rate of strength gain with time. The modality observed for ECC mixtures with the carbon-based materials can be due to significantly higher amounts of HRWR used in these mixtures compared to ECC-Control mixture as well. It should be emphasized that the differences in the compressive strength increment rates of ECC mixtures with extended curing ages are also related to the large differences in the 7-day results which lower the strength gain rates for mixtures with carbon-based materials.

Addition of carbon-based materials generally improved the compressive strength results (Fig. 3). The observed behavior was especially more pronounced at the early ages. For example, average 7-day compressive strength result of ECC-Control mixture was 27.5 MPa while with the addition of CF, CNT and CB, similar same-age values increased to 39.2, 47.7 and 42.4 MPa, respectively. Beyond 7 days, the differences in the compressive strength results of mixtures with and without carbon-based materials were not that significant suggesting that, in terms of compressive strength development, the addition of carbon-based fillers (especially those at nano-scale) is effective during the early stages of hydration. Similar results were also reported in the literature both for carbon-based materials [26] and different nano materials such as nano-silica and nano-calcite [38–40].

CNT was the best in enhancing the compressive strength results of ECC-Control for all curing ages (Fig. 3). The effectiveness of CF and CB on compressive strength results was variant and dependent on the curing age. All carbon-based materials used in this study are inert which means that they do not directly participate in hydration/pozzolanic reactions of the cementitious pastes. It is thus rational to state that rather than stimulating the hydration/pozzolanic capability of cementitious ingredients, thanks to their contributions to provide additional nucleation sites (due to significantly high specific surface area) for the settlement of hydration products [26], compressive strength results of ECC-CNT spec-

imens were higher than other mixtures for all curing ages. CNT particles may have also acted physically in filling the pore network at nano-scale, especially the pores between calcium silicate hydrate (C-S-H) gels, calcium hydroxide (CH) and ettringite [41], or even by bridging the gel pores within C-S-H gels and resulting in enhancements in the stiffness of C–S–H gels [42,43]. It is also notable that the chemical bonding between the CNT particles and matrix which is likely to strengthen upon further curing (e.g. 180 days), can help with the increased compressive strength results for ECC-CNT by strongly bridging micro/nano scale flaws.

3.2. Self-Sensing behavior under uniaxial compressive loading

In Figs. 4–7, self-sensing behavior of cubic specimens of different mixtures which were subjected to uniaxial compressive loading was presented for different curing ages. For all self-sensing plots of the study, straight and dashed lines represented the changes in stress and FCER results with respect to deformation, respectively.

As Fig. 4 clearly demonstrates, ECC-Control specimens exhibited self-sensing responsiveness under uniaxial compression with different FCER levels after each testing age. This behavior of plain ECC-Control specimens can be attributed to the mobilization of unbounded water and dissolved ions in micro-pores with the application of electric field that can lead to a piezoresistive response due to spatial separation of conductive phases [22]. Unburnt carbon (loss on ignition) of PC and FA are also likely to play a certain role in the self-sensing capability of ECC-Control. However, ECC-Control specimens, in most cases, were not able to self-sense the compressive damage, from the very beginning of loading and high FCER results were recorded at very large deformations. This calls the effectiveness of self-sensing in ECC-Control specimens into question. FCER results varied depending on the curing periods for ECC-Control specimens. No electrical data could be recorded from 180-day-old ECC-Control specimens since the 2-probe AC resistivity meter stopped producing impedance results when the values exceeded 1 MΩ. This does not mean that 180-day-old specimens were not responsive to damage but it was not possible to record self-sensing data due to substantial increments in ER which may be partly related to the drying of already-dry ECC-Control specimens at 60 °C for 24 h. Although compressive loading works as a squeezing agent for microcracks, characteristics of microcracks formed in 180-day-old ECC-Control specimens under compression might have also played a certain role in dramatically increasing the FCER results and not being able to observe self-sensing behavior. Microcracks with larger widths contribute more to the increments in ER results [15,22,23,32]. When the initial curing age is extended, fracture toughness and chemical bonding between PVA fibers and cementitious matrix increase which increases the microcrack widths due to higher chance of damage/rupture of PVA fibers [11] and so as the ER results. These findings show that for self-sensing with greater efficiency irrespective of the effects of testing equipment, moisture state, age and loading conditions (as will be detailed), electrically-conductive materials need to be present in plain ECCs.

Addition of carbon-based materials positively affected the self-sensing behavior of ECC-Control specimens (Figs. 5–7). For a given curing age, there were significant differences between recorded FCER results for ECC specimens with carbon-based materials and those without due to the improvements of electrical conductivities. In most of the tests, FCER results of ECC mixtures with carbon-based materials were higher than that of ECC-Control mixture at the moment of failure, irrespective of the age and type of conductive material. Most specimens of ECC-CF, ECC-CNT and ECC-CB mixtures started to exhibit changes in ER results from "point zero" meaning that they were characterized with the better self-sensing

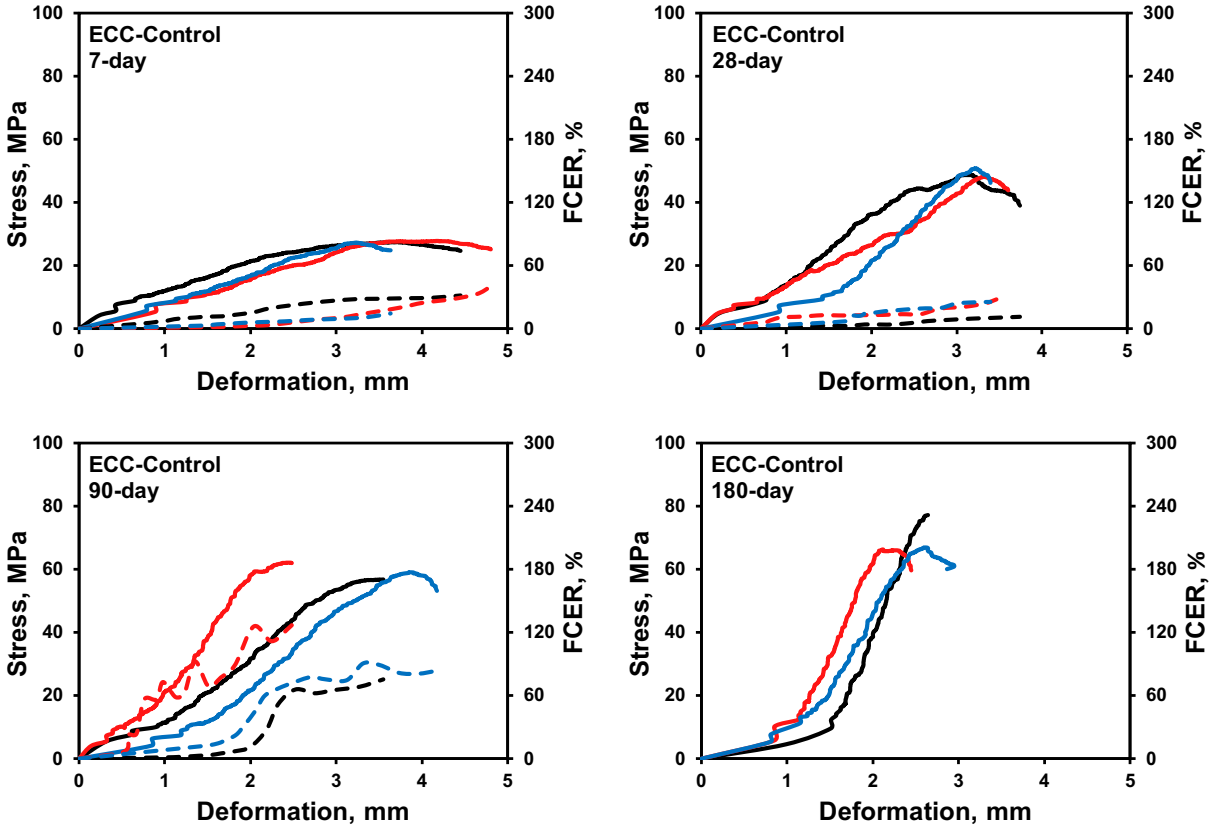

Fig. 4. Self-sensing behavior of different-age ECC-Control mixtures under uniaxial compression.

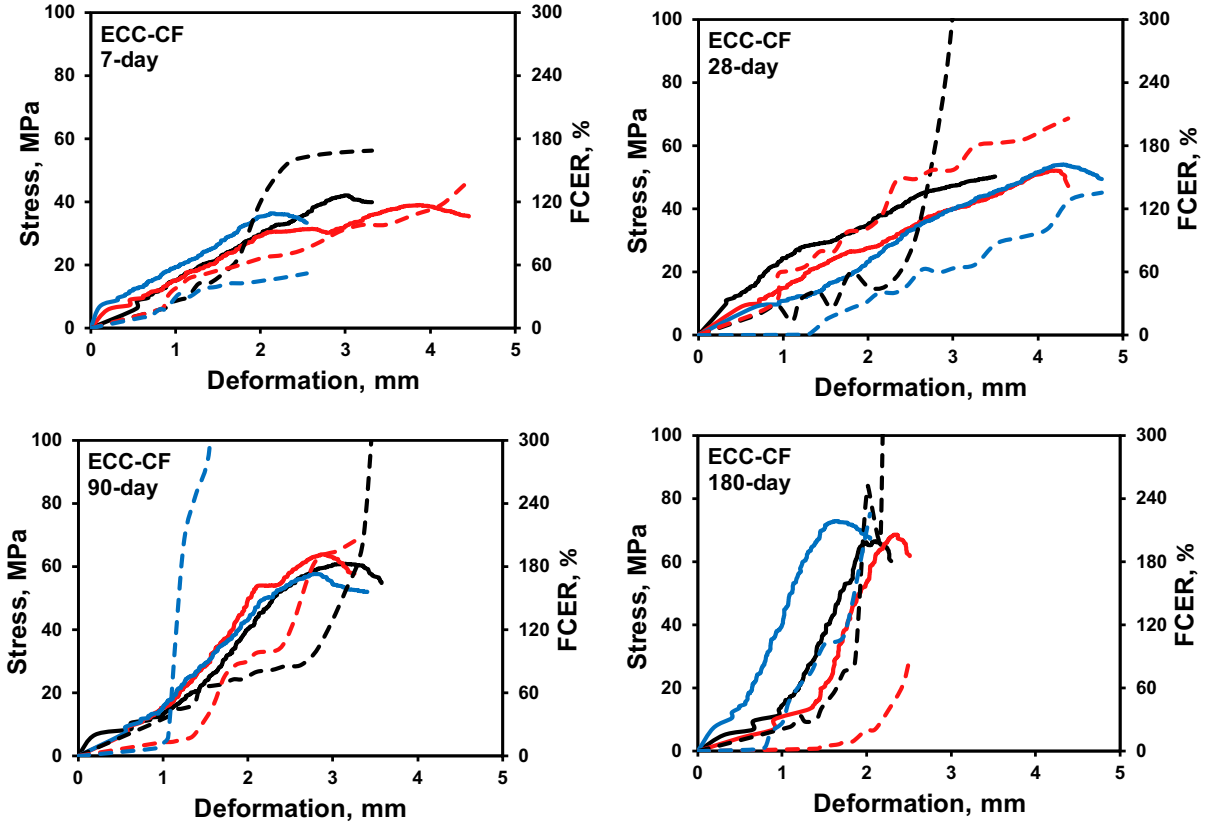

Fig. 5. Self-sensing behavior of different-age ECC-CF mixtures under uniaxial compression.

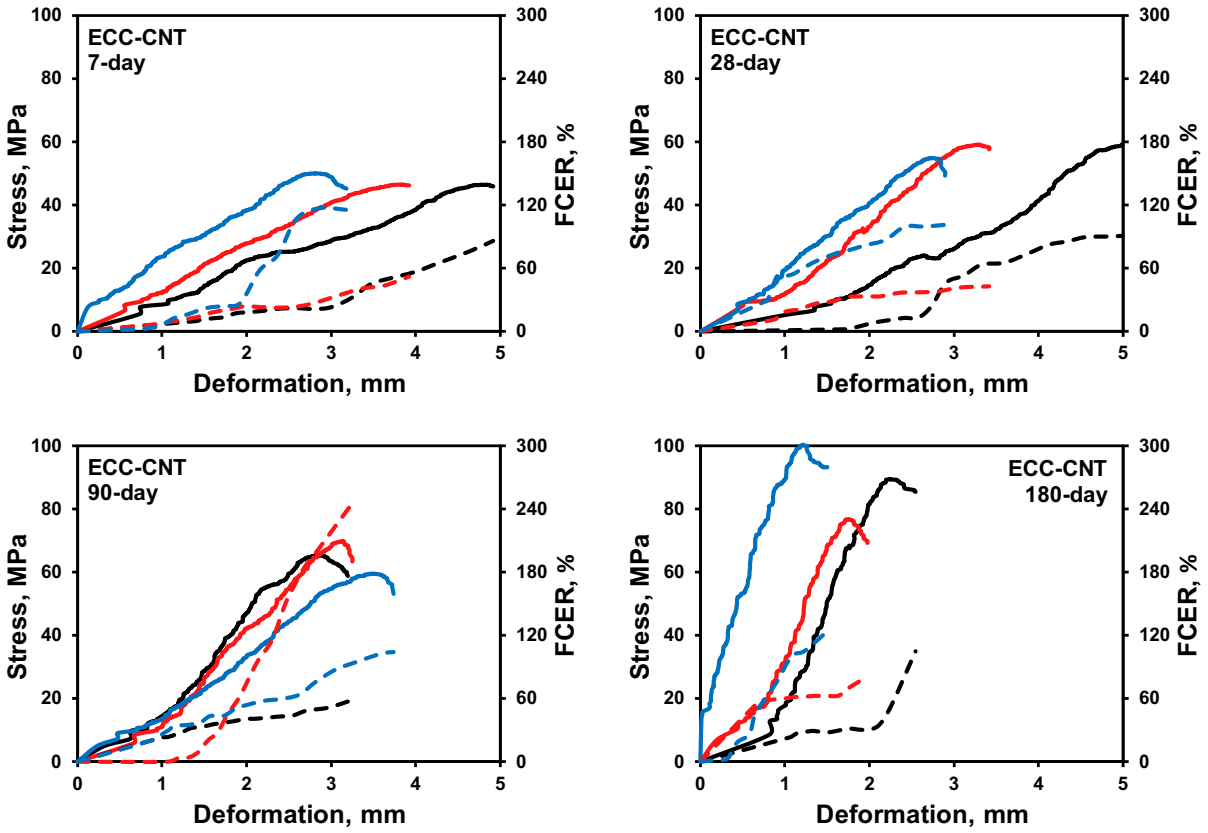

Fig. 6. Self-sensing behavior of different-age ECC-CNT mixtures under uniaxial compression.

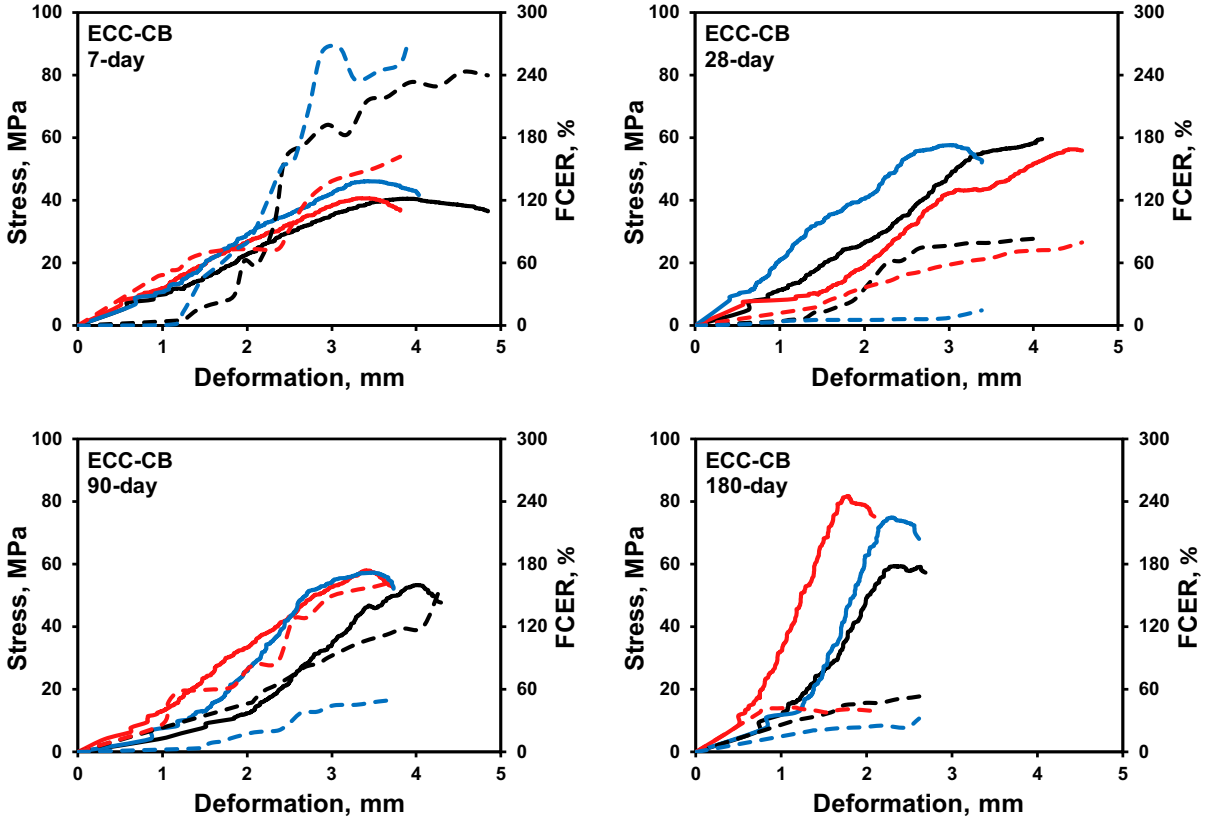

Fig. 7. Self-sensing behavior of different-age ECC-CB mixtures under uniaxial compression.

capability even at low imposed compressive damage. For certain ECC specimens at certain ages, self-sensing behavior was not that evident (with small changes in FCER results) when the level of compressive loading was low although improvements in the behavior were monitored when the level of loading increased. This might be related to the type of loading. At lower levels of deformation under compression, newly-formed microcracks are squeezed and specimens behave in a way that they were not deformed for a certain period of time and no dramatic increments in FCER results can be recorded. This argument becomes more logical when it is considered that the crack initiation in specimens tested under compression (especially for ECC specimens with high deformation capacity) is limited below 40–50% of the failure stress [44].

Utilization of CF made the best contribution to the self-sensing capability of ECCs. CF-based specimens were responsive to compressive damage starting from very small levels of deformation and this became much more pronounced (with much higher FCER results) upon progression in the loading (Fig. 5) which was also valid for all ages. The observed superiority of ECC-CF specimens in capturing electrical changes was attributed to the following: (i) higher aspect ratio of CF which increases the chance for edge-to-edge contact of discrete fibers and resultingly, the possibility to self-sense any disturbance (even the small deformations) that may occur in this well-linked electrically-conductive network [21], (ii) lower electrical resistivity of CF compared to other carbon-based materials [25,26] and (iii) possible and easier pull-out followed by rupture of CF during loading compared to other carbon-based materials of the study [44–46]. CNT and CB contributed similarly to the self-sensing (Figs. 6 and 7) after CF, although slightly larger FCER results were noted for ECC-CNT than ECC-CB specimens, especially at later ages. Similarities between the self-sensing performances of CNT- and CB-based ECC mixtures were reported previously [26] and it was adviced that while deciding desirable carbon-based materials to use in ECC systems for self-sensing purposes, factors such as production cost and ease of uniform dispersibility should be considered strictly along with their effects on electrical properties of composite materials [26,36].

Self-sensing was valid for all different-age ECC specimens (except 180-day-old ECC-Control) despite the one day drying of specimens at 60 °C prior to testing. Although comparable results were obtainable from late age specimens, self-sensing under compression was clearer for early age specimens. This can be associated with the significantly lower bulk ER results of ECC specimens at the early ages. Low early-age bulk ER results of specimens are linked with the availability of higher amounts of mixing water which did not participate in hydration/pozzolanic reactions, higher concentration/mobility of ionic species, less tortuous pore system and less dense hydration products which do not or limitedly interfere with the individual electrically-conductive materials [23,26,33]. When the initial ER results get lower, FCER results get higher resulting in clearer monitoring of deformation. Changes in self-sensing behavior are not restricted by the abovelisted parameters solely. The effects of these parameters are combined with the effects of elastic deformation of matrix, occurrence of new cracks, enlargement of previously-formed cracks, and crack propagation [33]. Although the effects of microcracking on the electrical properties of ECC are significant [15,22,23,32], due to type of loading discussed under this section, microcracks are expected to be squeezed and their effects, compared to tension-based loading conditions, are anticipated to be less pronounced. Therefore, modifications in self-sensing capability of different-age ECC specimens with regards to different microcracking characteristics were discussed in the following sections.

3.3. Mechanical behavior under splitting tensile loading

In Fig. 8-a and -b average splitting tensile strength and deformation results of ECC mixtures were shown for different initial curing ages, respectively. Curing age was influential on splitting tensile strength results. With extended curing, results increased for all mixtures in general. This finding which was also in line with the compressive strength results was anticipated since most parameters affecting the development of compressive strength with time also affect the strength measurements under tension-based loading conditions. However, it was notable that the rates of increment in 7-day splitting tensile strength results of mixtures were significantly more pronounced until the completion of 28 days (Fig. 8-a). This trend which was not observed for compressive strength may be related to more complex material properties (tensile first cracking strength, ultimate tensile strength and tensile strain capacity) affecting indirect tensile properties, particularly in the case of strain-hardening cementitious materials such as ECC [11]. Lower rates of increment in splitting tensile strength results of ECC mixtures with extended curing ages can be also associated with the consolidation of matrix and fiber-to-matrix interface properties.

Generally, addition of different types of carbon-based materials into ECC-Control mixture improved the splitting tensile strength results (Fig. 8-a), however, no distinctive trend for a certain carbon-based material (as in compressive strength) was notable, most probably due to abovementioned parameters affecting strength measurements under splitting tension.

Average splitting tensile deformation results of ECC mixtures were variant with respect to both different initial curing ages and types of carbon-based ingredients (Fig. 8-b). For all mixtures, splitting tensile deformation results increased from 7 to 28 days. When further cured for 90 and 180 days, results started to go down, especially for mixtures incorporated with the carbon-based materials (Fig. 8-b). In the case of ECC-like composites, certain decrements in deformation/strain results with time are expected [11,47]. Despite certain reductions, splitting tensile deformation results of ECC specimens incorporated especially with nano-scale carbon-based materials (CNT and CB) seem to stay around 1 mm even after 90 and 180 days (Fig. 8-b). Termination of further reductions in results of 90- and 180-day-old CNT- and CB-based ECC specimens may be associated with the balancing of fiber-to-matrix chemical and interfacial frictional bonding. Huang et al. [32] stated that when the amount of CB was increased in the ECC compositions, PVA fibers increasingly darkened due to absorption of CB by the fiber surfaces which resulted in stronger frictional bond strength increasing overall ductility via the formation of smaller-width microcracks under uniaxial tension which may also be the case here. Although extended curing is expected to increase fiber-to-matrix chemical bonding, the presence of nano-size carbon-based materials (CB and CNT) and their interaction with PVA fibers are likely to tailor the interfacial properties and account for increments in fiber-to-matrix chemical bonding by counterbalancing it with the frictional bond. For CF-based ECC mixtures, however, decrements in splitting tensile deformation results were continuously noted at extended ages (90 and 180 days) (Fig. 8-b) which may be related to the additional effects of CF in increasing the fiber-to-matrix chemical bonding in addition to the PVA fibers.

During splitting tensile loading, specimens are subjected to compressive stresses around areas very close to loading heads while large share of cross-sectional area out of the compression zone is subjected to the actions of tensile stresses. In this sense, embedment of brass electrodes (which may act like reinforcement) close to areas where changes in stress distributions occur (Fig. 2-b) is also likely to be effective in splitting tensile deformation results of ECC mixtures.

3.4. Self-Sensing behavior under splitting tensile loading

Self-sensing behavior of different-age individual specimens of ECC mixtures was shown in Figs. 9–12 for splitting tensile loading condition. For majority of self-sensing results recorded under splitting tension, the behavior clearly consisted of two parts. In the first part, while only minimal changes in FCER results were recordable, in the second part, sudden and incremental changes in FCER results were recorded. Sudden changes in FCER results mostly corresponded to the first humps (level of first cracking stress) that were observed in stress-deformation plots. Although multiple microcracks occurred in all ECC specimens loaded under splitting tension, self-sensing data were mostly represented as there was only a single crack formed and further enlarged over a selected specimen. This was associated with the proposed configuration used for self-sensing assessment under splitting tensile loading. As abovementioned, brass electrodes were inserted right at the top portion and 5 mm aside from the edges of cubic specimens (Fig. 2-b) meaning that only a limited area was observed for self-sensing. In this area of interest (between the opposite electrodes), there were both compressive and tensile stresses being effective although the area subjected to compression was less than that subjected to tension, due to nature of splitting tension test. Therefore, in this area, self-sensing data were not only influenced by the development of stresses with different origin but also by the cracking development. Noteworthy that deformability (cracking behavior) in this area is

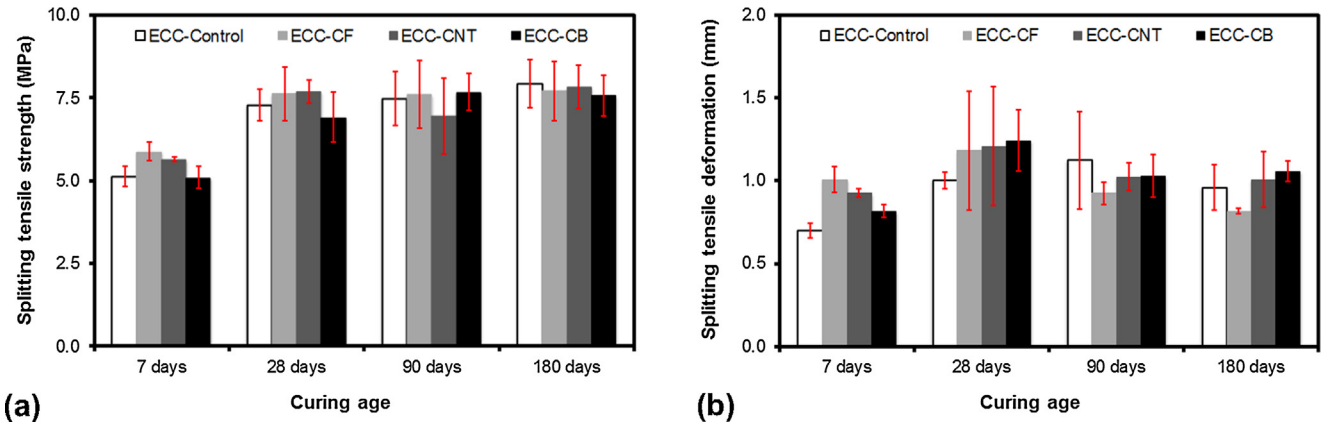

Fig. 8. Average (a) splitting tensile strength and (b) deformation results of different-age ECC mixtures. Error bars are according to standard deviations.

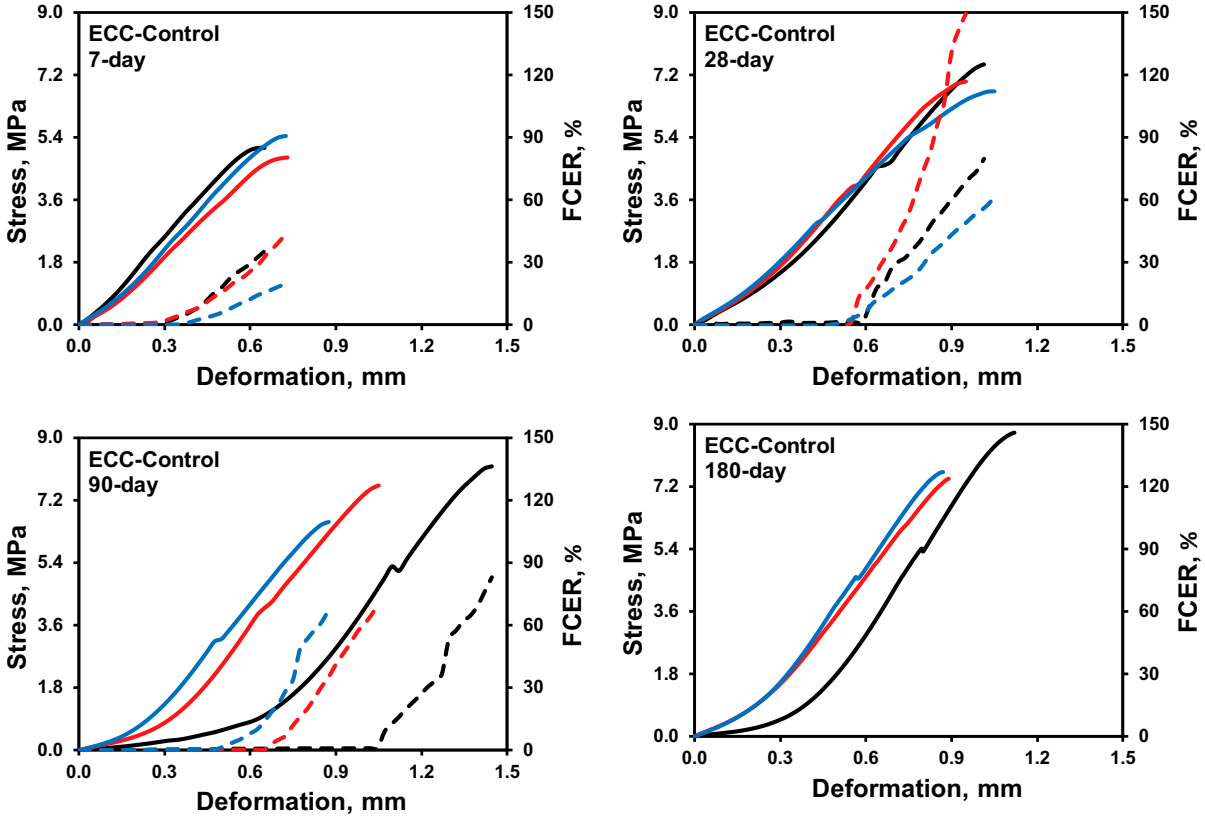

Fig. 9. Self-sensing behavior of different-age ECC-Control mixtures under splitting tension.

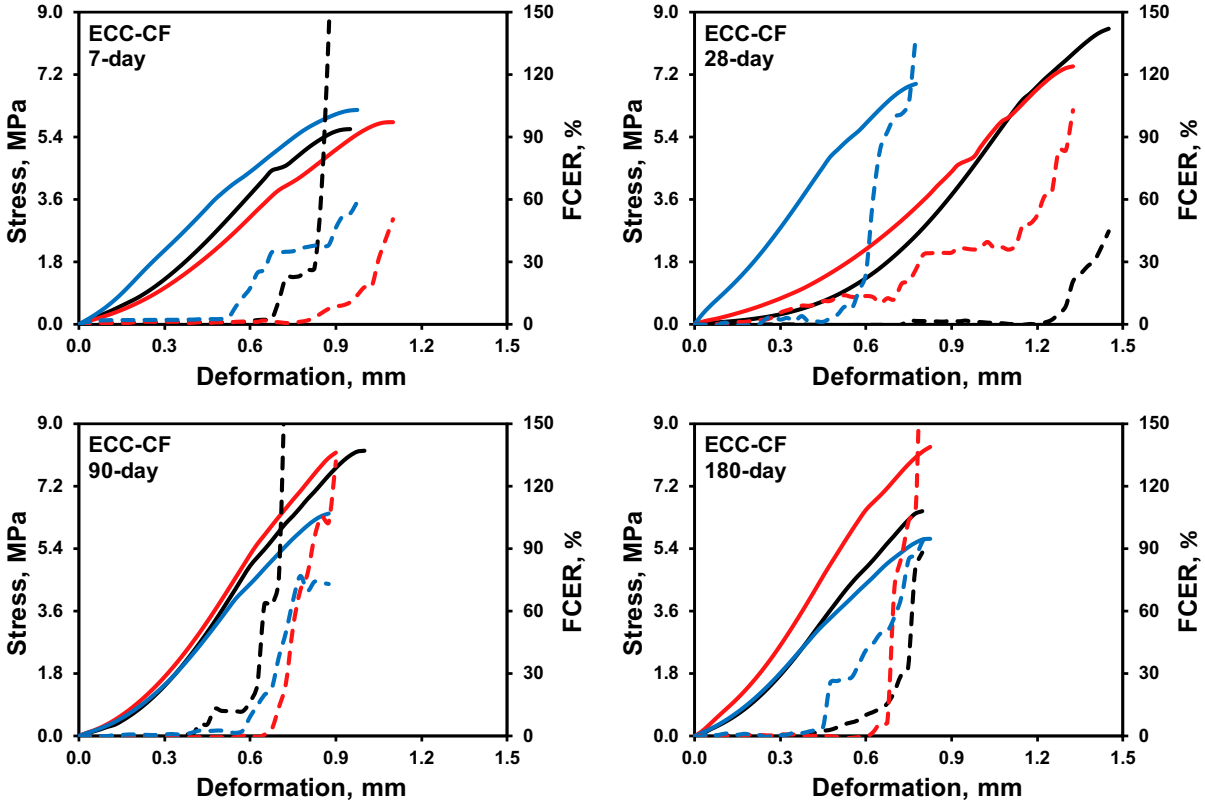

Fig. 10. Self-sensing behavior of different-age ECC-CF mixtures under splitting tension.

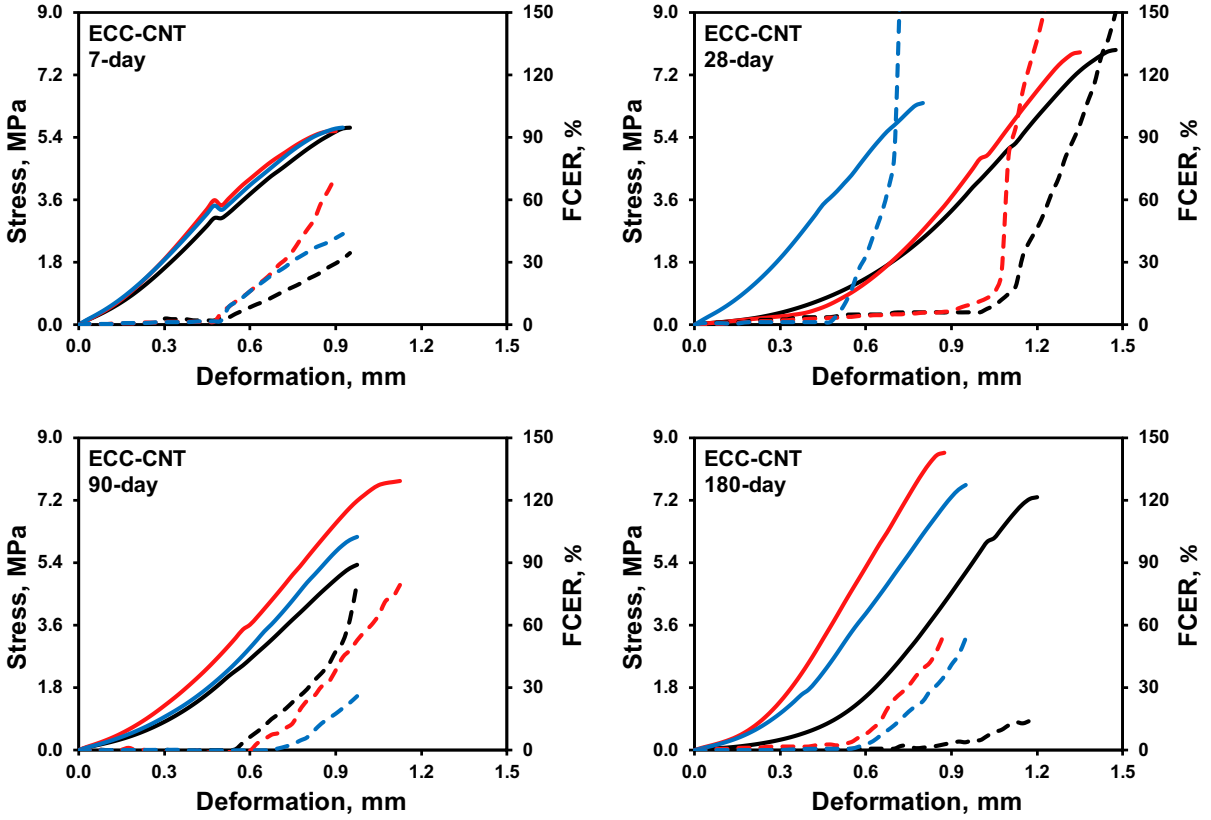

Fig. 11. Self-sensing behavior of different-age ECC-CNT mixtures under splitting tension.

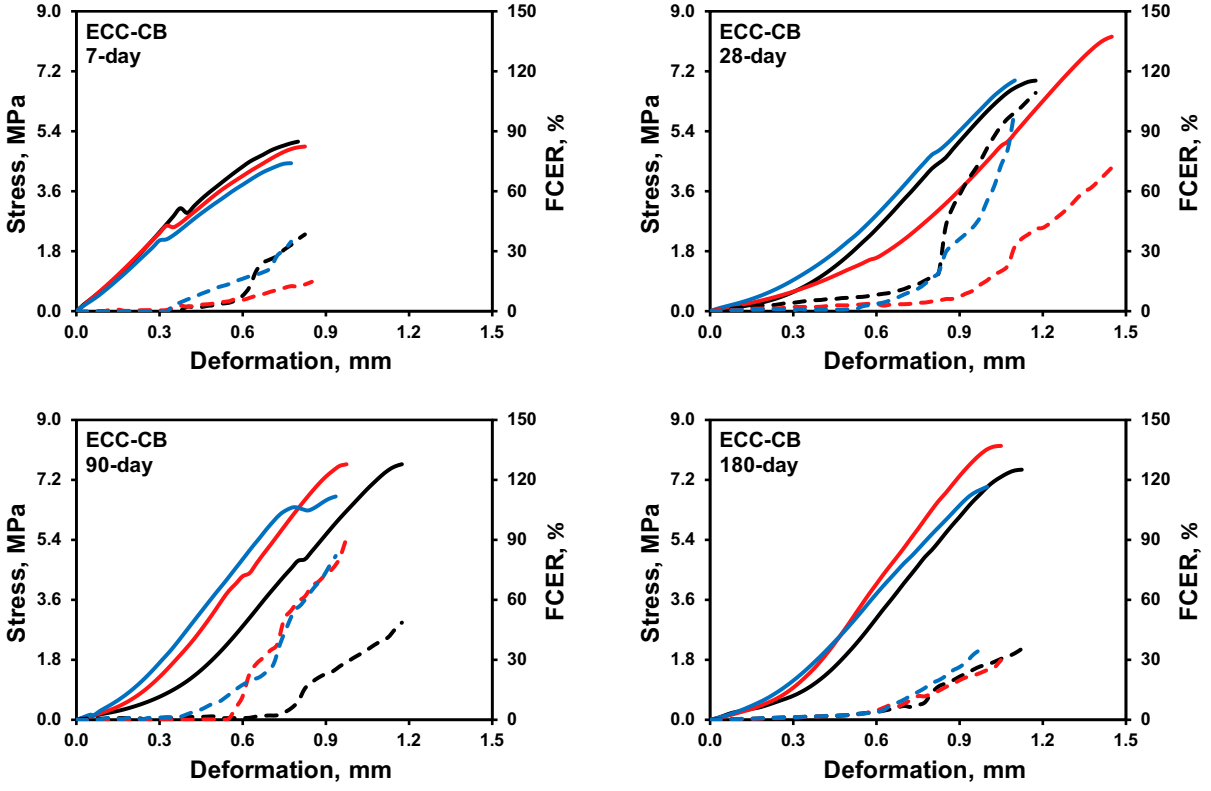

Fig. 12. Self-sensing behavior of different-age ECC-CB mixtures under splitting tension.

also influenced by the likelihood of brass electrodes to work similarly as steel reinforcement. Thus, minimal changes in FCER results until the first cracking region may be due to balancing of different types of stresses and corresponding deformations. Upon cracking either at areas close to specimen surfaces (top and bottom) or within the mid-space, FCER results started increasing and as cracks got together with further loading, they progressed with a larger energy towards the self-sensing area dramatically increasing FCER.

When incorporated with different carbon-based materials and tested for self-sensing under uniaxial compression, it was possible for ECC-Control specimens to improve self-sensing performance and become more vigilant to damage occurrences even at significantly small deformation levels (Figs. 4–7). However this was not the case for ECC-Control specimens tested under splitting tension (Figs. 9–12). Under splitting tension, the similar responsiveness was only slightly valid for selected ECC specimens with carbon-based materials and at certain ages (e.g. some of 28-day-old ECC specimens with CF, CNT and CB). These differences in contributions of carbon-based materials' on self-sensing of ECC systems under different loading scenarios were attributed to the differences in stress distributions arisen due to proposed testing configurations and microcracking behaviors. Clearer self-sensing plots with significantly higher FCER results were obtainable from ECC-CF specimens at the end of almost all predetermined ages (Fig. 10). Possible reasons for CF to better improve the self-sensing capability of ECC-Control specimens were already discussed under Section 3.2. CNT and CB contributed nearly the same to the self-sensing capability of ECC specimens tested under splitting tensile loading with slightly more FCER results acquired from ECC-CNT specimens at certain ages, in general (Figs. 11 and 12).

Self-sensing behavior under splitting tensile loading followed a similar trend to that observed under compressive loading with regards to aging. Splitting tensile deformation – FCER plots of 180-day-old ECC control specimens could not be drawn due to abrupt increments in ER measurements which exceeded the limit of 2-probe AC resistivity meter. All of the rest of the specimens were responsive to damage regardless of the initial curing age. When Figs. 4–7 and Figs. 9–12 are compared, it can be seen that at stress levels corresponding to level of first cracking, the jumps observed in FCER-deformation plots under splitting tension were much more pronounced than those observed under uniaxial compression. While mostly mild and continuous increments in FCER results were observable under compression, they were always very sudden and continuous under splitting tension. The observed differences in the self-sensing behavior were attributed to the differences in the effects of tension-originated microcracks which suddenly and more widely opened compared to compression-originated microcracks. Generally, self-sensing performance of splitting tensile damage was variable with better performance of early and mid age specimens (7, 28 and 90 days), however similarly successful measurements were also recorded after 180 days of curing depending on the type of carbon-based material and tested specimen (Figs. 9–12).

3.5. Mechanical behavior under four-point bending loading

Flexural tests were performed under continuous four-point bending loading and mechanical performance was investigated by average flexural strength and deformation results as well as observations made on individual stress-deformation plots. In Fig. 13, average flexural strength and deformation results of different-age ECC mixtures were shown. Flexural strength was calculated by using the maximum level of load recorded. Flexural deformation was the value corresponding to maximum level of flexural load which was used in flexural strength calculation.

For all ECC specimens, flexural strength results continuously increased with the increased curing ages as also reported for compressive and splitting tensile strength results (Fig. 13-a). Similar to splitting tensile strength, changes in flexural strength results with time were not that dramatic as in compressive strength results. Reasons that may cause for the observed behavior of different-age specimens were already discussed formerly, thus no additional statements were made here.

Effects of different carbon-based materials on flexural strength results of ECC mixtures were dependent on curing age. Addition of CF into ECC-Control specimens improved the flexural strength for all ages and CF was the best in improving flexural strength of control specimens among all carbon-based materials (Fig. 13-a). This was related with the increased amounts of fibers and in line with the literature [48,49]. Significantly higher elastic modulus (240 GPa) of CF than PVA fibers (42.8 GPa) might be also responsible for increased flexural strength results of ECC-CF specimens [49,50]. Age-dependent changes in flexural strength results of ECC-Control specimens became more evident in the case of CNT and CB utilization. Average 7-day flexural strength results of both ECC-CNT and ECC-CB specimens were found to be less than that of ECC-Control mixture. Average 28-day flexural strentgth result of ECC-CB specimens was less than that of ECC-Control mixture, as well. However, CNT- and CB-based specimens attained very similar and/or higher flexural strength results than that of ECC-Control after 90 and 180 days. Although the observed behavior of early age CB- and CNT-based ECC specimens can be related to more complex material properties affecting flexural strength development (see Section 3.3), significantly higher amounts of HRWR utilized for ECC-CNT and ECC-CB mixtures (Table 2) are also believed to be effective. Increased HRWR amounts, especially at early ages, are

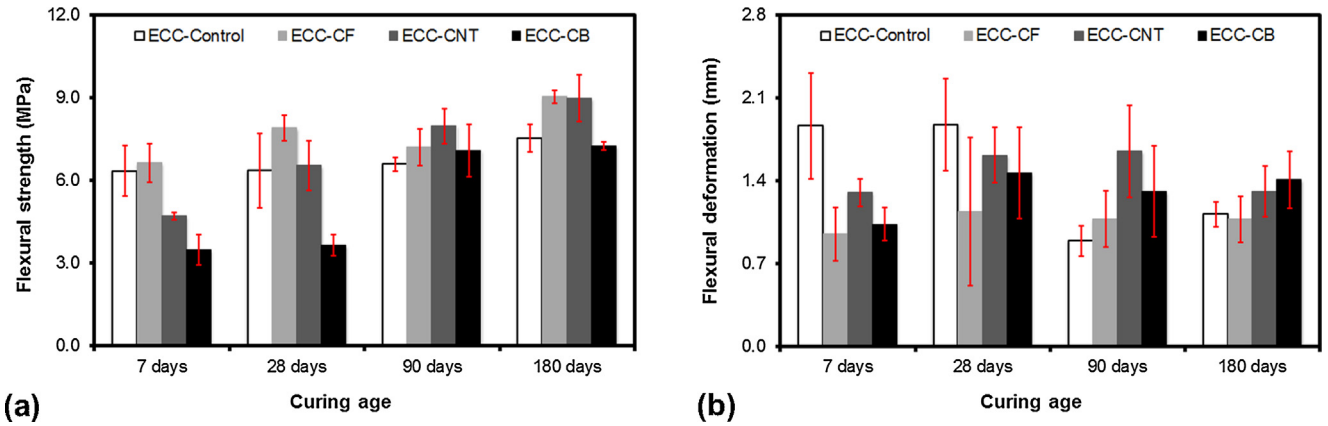

Fig. 13. Average (a) flexural strength and (b) deformation results of different-age ECC mixtures. Error bars are according to standard deviations.

very likely to delay the improvements that would normally take place in the interface properties between the fibers and cementitious matrix and thus in flexural strength results. Certain levels of loss in flexural strength results when CB and CNT were included in plain ECC mixtures were also noted in the literature [21,36,51]. Despite certain reductions recorded, some of individual specimens of ECC-CNT and ECC-CB mixtures exhibited similar flexural strength results to that of ECC-Control mixture.

Average flexural deformation results of ECC mixtures were changeable depending on the curing age and type of carbon-based materials (Fig. 13-b) and were mainly in line with the general trend observed for splitting tensile deformation results with minor behavioral differences. The values clearly decreased with prolonged curing in the case of ECC-Control mixture. However, for CNT- and CB-based specimens, flexural deformation results recorded at the early ages increased at later ages. For ECC-CF specimens, similar increments in flexural deformation results of specimens with time were not that evident. Although they were recorded under uniaxial tension, compared to plain ECC mixtures without any carbon-based materials, reductions in tensile strength and strain results were also recorded for ECC-CB specimens in the recent literature studies [24,30,32].

Deflection-hardening behavior is confirmed if the peak flexural load and its corresponding deformation are greater than the first cracking load and its corresponding flexural deformation, respectively. By further increasing the gap between the load at the first cracking/peak and deformation at the first cracking/peak load, deflection-hardening behavior can be improved [48]. Deflection-hardening response which is regularly displayed by ECC-Control was also valid for ECC-CF, ECC-CNT and ECC-CB specimens (Figs. 14–17) and it was significantly improved in the presence of nano-size carbon-based materials especially at curing ages of 90 and 180 days.

3.6. Self-Sensing behavior under four-point bending loading

Self-sensing results which were recorded under four-point bending were shown in Figs. 14–17. Self-sensing plots included in these figures can be interpreted in three parts with respective changes against flexural stress – deformation plots. The first part consists of the area starting with the initiation of flexural loading until the creation of first cracking where the linearity of flexural stress – deformation plot is valid (elastic stage). The second part starts from the first cracking and is accompanied by deflection-hardening process coupled with multiple microcracking. The third part can be considered as the deflection-softening area where sudden drop in the flexural load carrying capacity is observed due to localization of a certain microcrack leading to final failure. The general view regarding the FCER – deformation plots of ECC specimens was that during the elastic stage until the first cracking, FCER results increased although these were minimal. At the elastic stage where no visible microcracks are available, the observed slight changes in FCER results may be attributed to the charging of individual carbon-based materials and/or electrically-conductive phases of specimens subjected to flexural loading [36]. Increments in FCER results within the elastic stage can be also related to the polarization phenomenon [36,45,52]. Another reason for the observed increments of FCER results within the elastic stage can be the presence of microcracks in the interfacial transition zones existing between the matrix and aggregate, even before the start of flexural loading [36]. According to [53], the width, length and number of these microcracks start to increase after loading. As can be seen from Figs. 14–17 that for almost all specimens of different ECC mixtures, level of flexural loading (stress) reached up to half of the ultimate point within the elastic stage (until first cracking point) which is very likely to change the stability state of interfacial transition zone and increase FCER results. Regarding

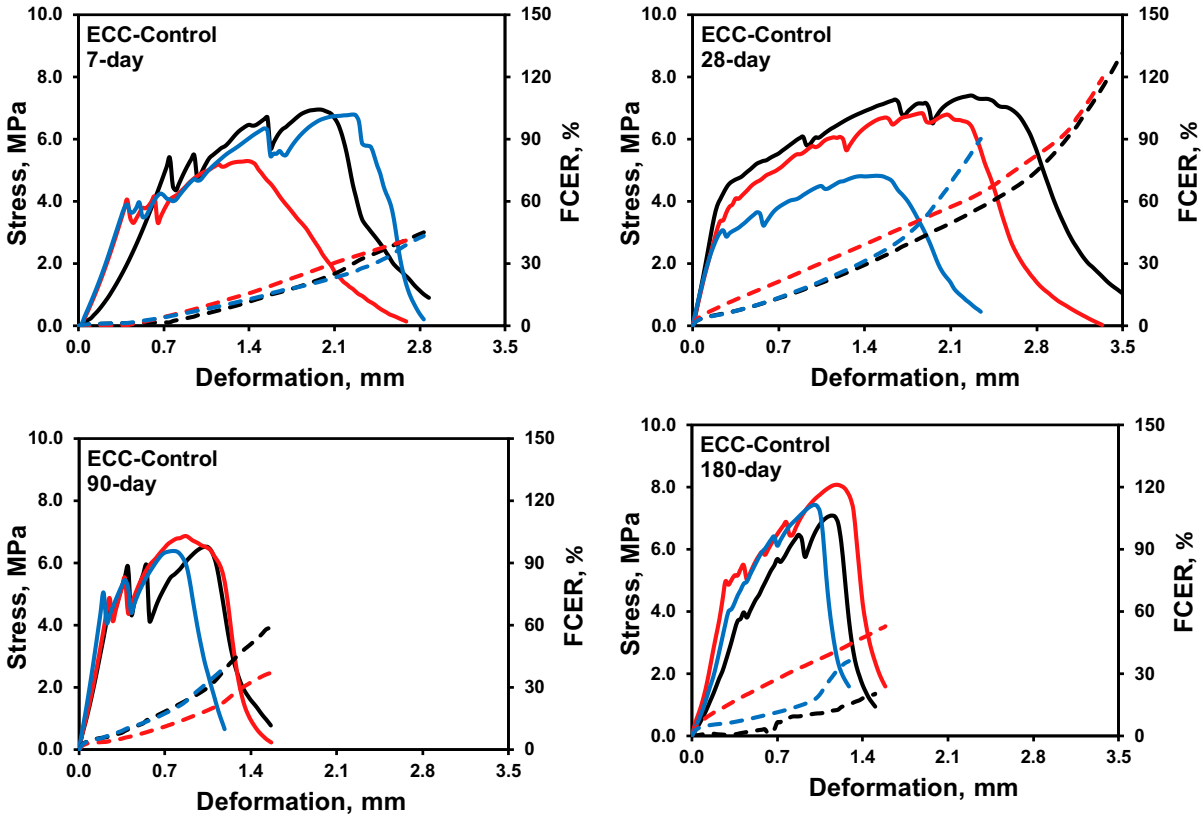

Fig. 14. Self-sensing behavior of different-age ECC-Control mixtures under four-point bending.

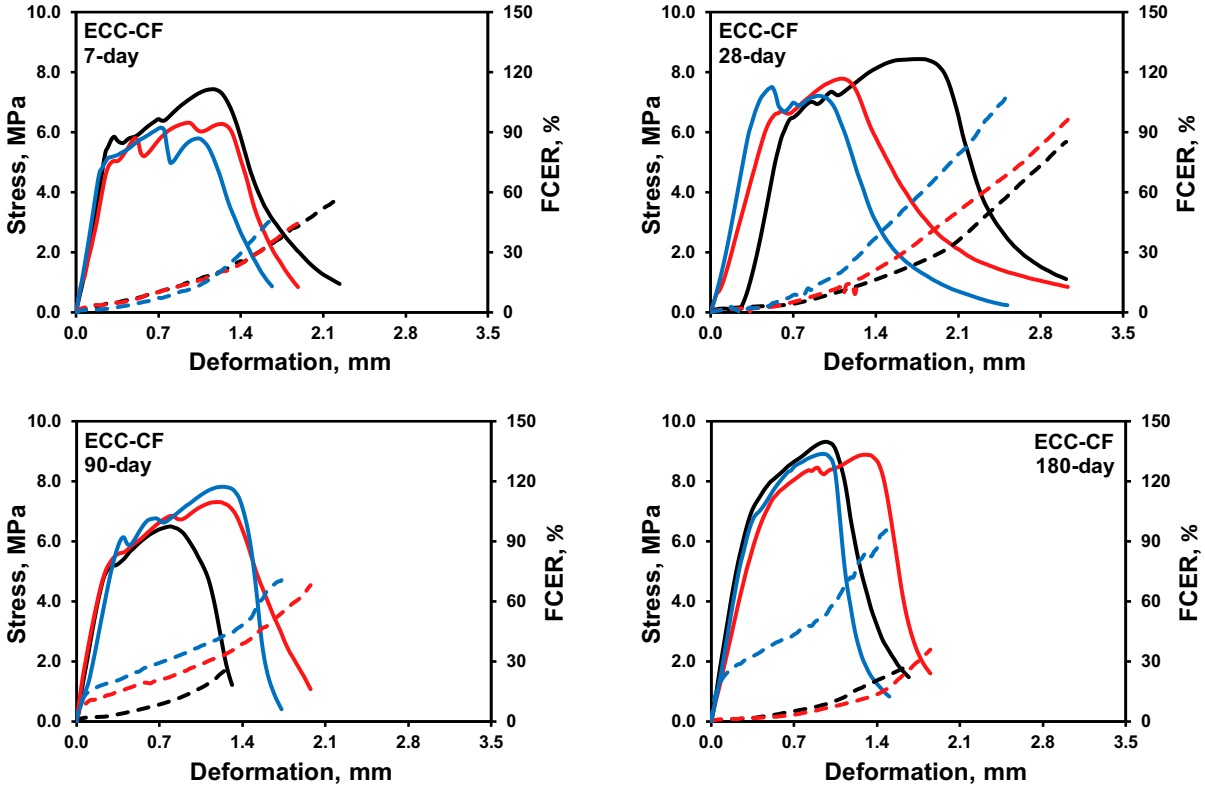

Fig. 15. Self-sensing behavior of different-age ECC-CF mixtures under four-point bending.

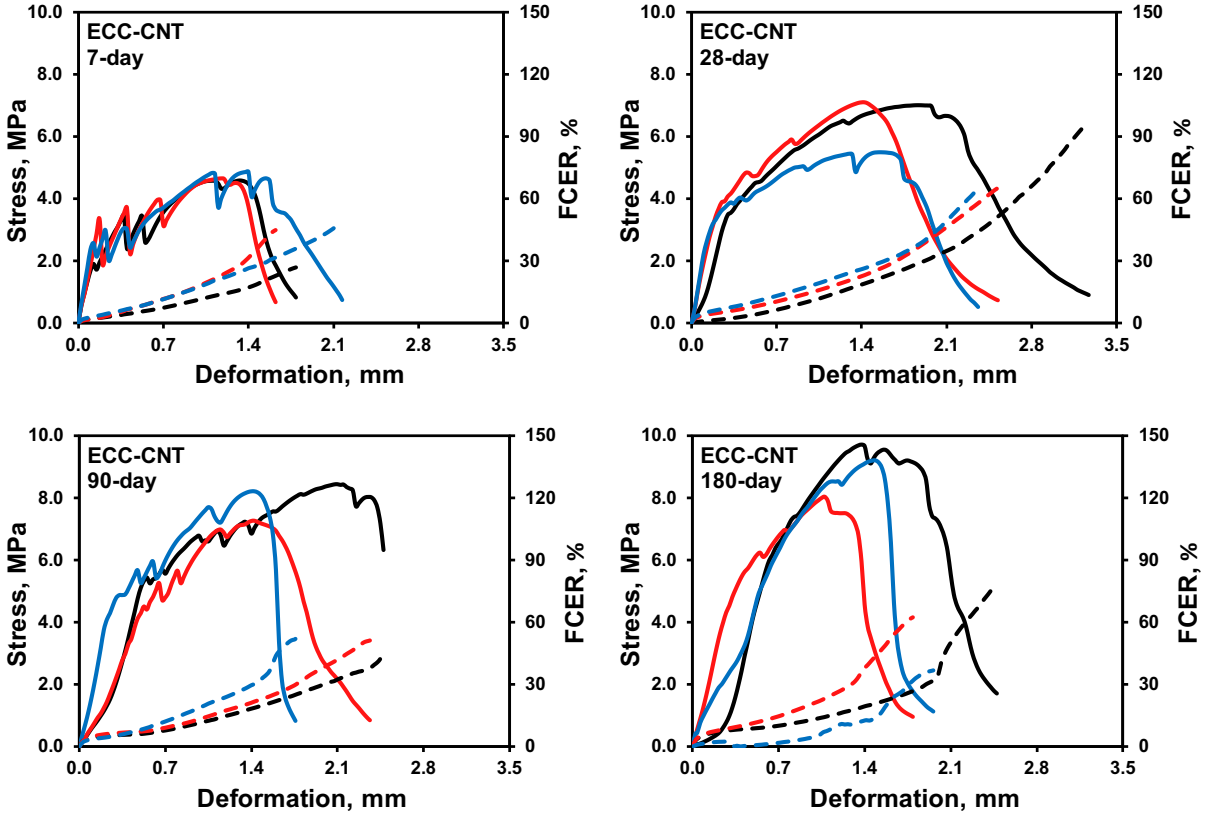

Fig. 16. Self-sensing behavior of different-age ECC-CNT mixtures under four-point bending.

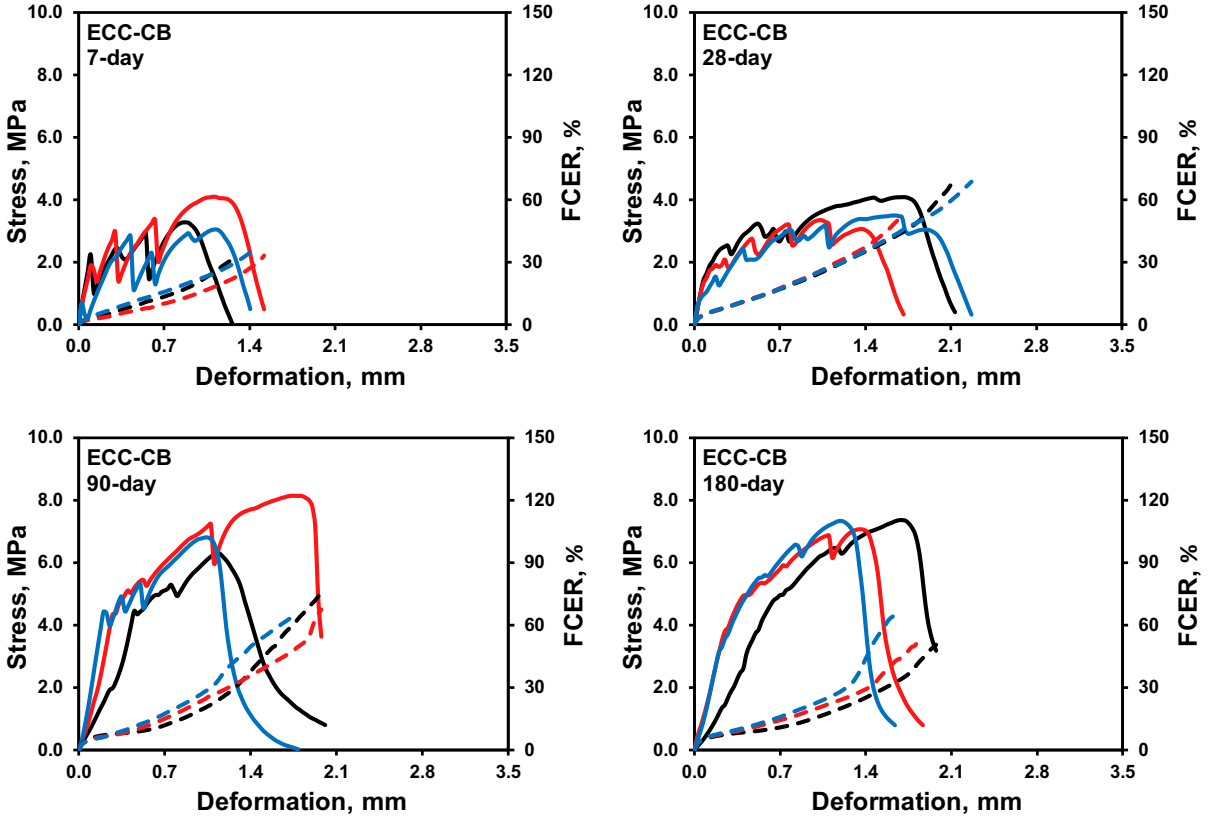

Fig. 17. Self-sensing behavior of different-age ECC-CB mixtures under four-point bending.

the FCER observations made for elastic region, similar findings were also reported in the the study of Li et al. [31] which tested CB-based ECC coupon specimens under uniaxial tension and concluded that this might be due to the change in the energy band gap between its valence and conductive band at low strain levels [54].

As the level of flexural loading increased and deflection-hardening is experienced, FCER results continuously increased for all mixtures irrespective of the curing age due to separation and/or break-down of conductive paths due to microcracking. Continuous increments in FCER during the deflection-hardening were followed by more dramatic escalations at stress close to final failure most probably due to localization of a certain microcrack. The mild incremental trend in FCER results with progressive flexural loading was found to be similar to that observed under uniaxial compression, most probably due to the distance between electrodes' location (Fig. 2) and expected microcracking area (right under the upper loading heads) of prismatic specimens.

Although carbon-based materials were effective on self-sensing under flexure, their respective effect was not enough to create a general trend. In broad sense, FCER results of ECC-Control specimens during deflection-hardening and deflection-softening/failure parts of flexural deformation are mainly related to the formation of microcracks and their enlargement/propagation (Fig. 14). Along with the characteristics of microcracks, changes in FCER results of ECC-CF, ECC-CNT and ECC-CB specimens are also expected to be influenced by the presence of different carbon-based materials either directly bridging the microcracks and/or help contribute the bridging of PVA fibers by attaching on their surfaces. Although higher FCER results help better visualization of self-sensing, FCER results of ECC specimens with carbon-based materials were mostly similar or less than ECC-Control. Especially the changes in FCER results of ECC-CF specimens (Fig. 15) were similar to that of ECC-Control while specimens with CNT and CB exhibited slightly less pronounced FCER increments at the end of specified curing ages compared to ECC-Control. In the incident of microcracking and further progression, FCER results increase and if carbon-based materials bridging the microcracks are not available or small in number, FCER results similar to ECC-Control can be expected. The behavior noted for ECC-CF specimens can thus, be attributed to the tendency of CF to more easily pull-out/break and not being able to help create microcracks with smaller widths under flexure as also evidenced from lower flexural deformation results (Fig. 13-b) [21,51]. For ECC-CNT and ECC-CB specimens (Figs. 16 and 17), slightly less pronounced FCER increments than ECC-Control specimens can be attributed to the capability of individual CNT and CB particles to bridge microcracks and/or be attached over PVA fibers in addition to higher flexural deformation results (Fig. 13-b) especially at later ages triggering more multiple microcracks with smaller widths. It is notable that easier pull-out/breakage tendency of CF at higher levels of loading may not be desirable if reversibility in electrical properties is necessary as in the case of structures subjected to cyclic loading conditions such as transport structures [21,51,55]. Thus, the decision-making of selection of carbon-based materials and fracture toughness of matrices should be carefully engineered to eliminate any possible drawbacks regarding excessive mechanical loading and proper response for a certain self-sensing need.

Self-sensing of flexural damage was valid for all curing ages and specimens of different ECC mixtures. Different from results obtained under uniaxial compression and splitting tension, it was possible to record the FCER results of 180-day-old ECC-Control specimens under flexure (Fig. 14). This was not only related to the selection of different devices to record ER but also to the exten-

sion of microcracks of failed specimens over a larger span and farther positioning of electrodes with respect to microcracks (Fig. 2-c). When different-age specimens manufactured from completely different ECC compositions and tested under different loading conditions are considered, it can be stated that in order not for electrical recordings to be restricted by the testing equipment, aging, moisture state, general microcracking characteristics and position of electrodes, electrically conductive fillers must be included in ECC compositions for sufficient electrical conductivity.

4. Conclusions

A comprehensive study was undertaken in which the self-sensing capability together with the mechanical properties of Engineered Cementitious Composites (ECC) with different carbon-based materials was evaluated after initial curing periods of 7, 28, 90 and 180 days and when loaded under uniaxial compression, splitting tension and four-point bending. Following conclusions were drawn:

- Self-sensing capability of ECC-Control specimens was significantly improved with the addition of carbon-based materials within the mixtures' compositions although the extent of improvements was dependent on loading conditions and aging of specimens. Carbon-based materials made the most evident contributions in self-sensing capability of specimens tested under uniaxial compression, especially at early ages of initial curing. It seems that characteristics of microcracks, ability of individual carbon-based materials to contribute microcrack bridging, testing configuration and measurement device are the factors markedly affecting the self-sensing capability of ECC mixtures irrespective of the proposed loading conditions.
- Regardless of the loading conditions and curing ages, CF-based ECC specimens exhibited the most clear self-sensing behaviors as realized by significantly higher FCER results, in general. This behavior was not only related to the lower initial resistivity values of ECC-CF specimens but also to the effects of overall microcracking behavior and pull-out/breakage of individual CF as a consequence of loading. The self-sensing performance of CNT- and CB-based ECC specimens were found to be similar although FCER results recorded for these specimens were not as high as ECC-CF specimens mostly. Utilization of CNT and CB is suggested over CF for self-sensing purposes in ECC, if reversibility in self-sensing is desirable.
- All different-age specimens from different ECC mixtures were responsive to damage under different loading types showing the validity of self-sensing. However, it was not possible to comment on the self-sensing behavior of 180-day-old ECC-Control specimens tested under uniaxial compression and splitting tension due to limitations of 2-probe AC resistivity meter. This therefore clearly showed that although ECC-Control specimens were responsive to damage occurrence under all proposed loading conditions (with significantly lower FCER results under certain conditions), it is necessary to further reduce the bulk resistivity of materials with the help of certain electrically-conductive materials in order not to be restricted by aging, testing configuration/equipment, loading conditions, microcrack characteristics etc.
- Inclusion of different carbon-based materials within the ECC-Control mixture generally improved the mechanical properties of specimens, however, the levels of improvement were dependent on the loading condition, curing age and type of carbon-based materials. While clear increments in compressive strength of ECC-Control specimens were noted in the presence of all carbon-based materials, this was not always the case for parameters calculated under splitting tensile and four-point bending loading. This discrepancy in the mechanical results was attributed to different testing configurations and factors being influential on individual test results.

Declaration of Competing Interest

The authors declare that they have no known competing financial interests or personal relationships that could have appeared to influence the work reported in this paper.

Acknowledgements

The authors gratefully acknowledge the financial assistance of the Scientific and Technical Research Council (TUBITAK) of Turkey provided under project: 114R043.

References

[1] G. Yıldırım, Dimensional stability of deflection-hardening hybrid fiber reinforced concretes with coarse aggregate: suppressing restrained shrinkage cracking, Struct. Concr. 20 (2019) 836–850.
[2] M. Şahmaran, Ö. Anıl, M. Lachemi, G. Yıldırım, A.F. Ashour, F. Acar, Effect of corrosion on shear behavior of reinforced engineered cementitious composite beams, ACI Struct. J. 112 (2015) 771–782.
[3] A. Alyousif, M. Lachemi, G. Yıldırım, G.H. Aras, M. Şahmaran, Influence of cyclic frost deterioration on water sorptivity of microcracked cementitious composites, J. Mater. Civ. Eng. 28 (2015) 04015159.
[4] V.C. Li, Engineered Cementitious Composites – tailored composites through micromechanical modeling in fiber reinforced concrete: present and the future, in: N. Banthia, A. Bentur, A. Mufti (Eds.), Cdn. Society of Civil Eng., 1998, pp. 64–97.
[5] G. Yıldırım, M. Şahmaran, M.K.M. Al-Emam, R.K.H. Hameed, Y. Al-Najjar, M. Lachemi, Effects of compressive strength, autogenous shrinkage and testing methods on the bond behavior of HES-ECC, ACI Mater. J. 112 (2015) 409–418.
[6] A. Alyousif, Ö. Anıl, M. Şahmaran, M. Lachemi, G. Yıldırım, A.F. Ashour, Comparison of shear behavior of engineered cementitious composite and normal concrete beams with different shear span lengths, Mag. Concr. Res. 68 (2015) 217–228.
[7] Y. Al-Najjar, S. Yeşilmen, A. Al-Dahawi, M. Şahmaran, G. Yıldırım, M. Lachemi, L. Amleh, Physical and chemical actions of nano-mineral additives on properties of high-volume fly ash Engineered Cementitious Composites, ACI Mater. J. 113 (2016) 791–801.
[8] M. Şahmaran, H.E. Yücel, G. Yıldırım, M. Al-Emam, M. Lachemi, Investigation of the bond between concrete substrate and ECC overlays, J. of Mater. Civil Eng. 26 (2013) 167–174.
[9] V.C. Li, High-performance and multifunctional cement-based composite material, Engineering 5 (2019) 250–260.
[10] H. Liu, Q. Zhang, V.C. Li, H. Su, C. Gu, Durability study on Engineered Cementitious Composites (ECC) under sulfate and chloride environment, Constr. Build. Mater. 133 (2017) 171–181.
[11] M. Şahmaran, G. Yıldırım, T.K. Erdem, Self-healing capability of cementitious composites incorporating different supplementary cementitious materials, Cem. Concr. Compos. 35 (1) (2013) 89–101.
[12] M. Şahmaran, V.C. Li, Suppressing alkali-silica expansion, Concr. Int. 38 (5) (2016) 47–52.
[13] G. Yıldırım, Ö.K. Keskin, S.B. Keskin, M. Şahmaran, M. Lachemi, A review of intrinsic self-healing capability of Engineered Cementitious Composites: recovery of transport and mechanical properties, Constr. Build. Mater. 101 (2015) 10–21.
[14] G. Yıldırım, M. Şahmaran, H.U. Ahmed, Influence of hydrated lime addition on the self-healing capability of high-volume fly ash incorporated cementitious composites, J. Mater. Civ. Eng. 27 (6) (2015) 04014187.
[15] M. Şahmaran, G. Yıldırım, G.H. Aras, S.B. Keskin, Ö.K. Keskin, M. Lachemi, Self-healing of cementitious composites to reduce high CO2 emissions, ACI Mater. J. 114 (1) (2017) 93–104.
[16] G. Yıldırım, A. Alyousif, M. Şahmaran, M. Lachemi, Assessing the self-healing capability of cementitious composites under increasing sustained loading, Adv. Cem. Res. 27 (10) (2015) 581–592.
[17] A. Alyousif, M. Lachemi, G. Yıldırım, M. Şahmaran, Effect of self-healing on the different transport properties of cementitious composites, J. Adv. Concr. Tech. 13 (3) (2015) 112–123.
[18] G. Yıldırım, M. Şahmaran, M. Balçıkanlı, E. Özbay, M. Lachemi, Influence of cracking and healing on the gas permeability of cementitious composites, Constr. Build. Mater. 85 (2015) 217–226.
[19] M. Şahmaran, G. Yıldırım, R. Noori, E. Özbay, M. Lachemi, Repeatability and pervasiveness of self-healing in Engineered Cementitious Composites, ACI Mater. J. 112 (4) (2015) 513–522.

[20] G. Yıldırım, A.H. Khiavi, S. Yeşilmen, M. Şahmaran, Self-healing performance of aged cementitious composites, Cem. Concr. Compos. 87 (2018) 172–186.
[21] G. Yıldırım, M.H. Sarwary, A. Al-Dahawi, O. Öztürk, Ö. Anıl, M. Şahmaran, Piezoresistive behavior of CF-and CNT-based reinforced concrete beams subjected to static flexural loading: shear failure investigation, Constr. Build. Mater. 168 (2018) 266–279.
[22] R. Ranade, J. Zhang, J.P. Lynch, V.C. Li, Influence of micro-cracking on the composite resistivity of Engineered Cementitious Composites, Cem. Concr. Res. 58 (2014) 1–12.
[23] G. Yıldırım, G.H. Aras, Q.S. Banyhussan, M. Şahmaran, M. Lachemi, Estimating the self-healing capability of cementitious composites through non-destructive electrical-based monitoring, NDT & E. Int. 76 (2015) 26–37.
[24] H. Deng, H. Li, Assessment of self-sensing capability of carbon black Engineered Cementitious Composites, Constr. Build. Mater. 173 (2018) 1–9.
[25] A. Al-Dahawi, O. Öztürk, F. Emami, G. Yıldırım, M. Şahmaran, Effect of mixing methods on the electrical properties of cementitious composites incorporating different carbon-based materials, Constr. Build. Mater. 104 (2016) 160–168.
[26] A. Al-Dahawi, M.H. Sarwary, O. Öztürk, G. Yıldırım, A. Akın, M. Şahmaran, M. Lachemi, Electrical percolation threshold of cementitious composites possessing self-sensing functionality incorporating different carbon-based materials, Smart Mater. Struct. 25 (10) (2016) 105005.
[27] X. Fu, D.D.L. Chung, Effect of curing age on the self-monitoring behavior of carbon fiber reinforced mortar, Cem. Concr. Res. 27 (9) (1997) 1313–1318.
[28] T.C. Hou, J.P. Lynch, Tomographic imaging of crack damage in cementitious structural components, in: Proceedings of the 4th International Conference on Earthquake Engineering, Taipei, China, 2006, p. 162.
[29] T.C. Hou, J.P. Lynch, Conductivity-based strain monitoring and damage characterization of fiber reinforced cementitious structural components, in: Proceedings of SPIE 12th Annual International Symposium on Smart Structures and Materials, San Diego, 2005, pp. 419–429.
[30] V.W.J. Lin, M. Li, J.P. Lynch, V.C. Li, Mechanical and electrical characterization of self-sensing carbon black ECC, in: Proceedings of SPIE, The Inter. Soc. Opt. Eng., 2011, pp. 1–12.
[31] M. Li, V.W.J. Lin, J.P. Lynch, V.C. Li, Carbon black Engineered Cementitious Composites-mechanical and electrical characterization, ACI Spec. Publ. 292 (2013) 1–16.
[32] Y. Huang, H. Li, S. Qian, Self-sensing properties of Engineered Cementitious Composites, Constr. Build. Mater. 174 (2018) 253–262.
[33] M. Li, V. Lin, J. Lynch, V.C. Li, Multifunctional carbon black Engineered Cementitious Composites for the protection of critical infrastructure, in: High Performance Fiber Reinforced Cement Composites RILEM Bookseries, Springer, Dordrecht, 2012, pp. 99–106.
[34] B. Suryanto, W.J. McCarter, G. Starrs, S.A. Wilson, R.M. Traynor, Smart cement composites for durable and intelligent infrastructure, Procedia Eng. 125 (2015) 796–803.
[35] H. Li, J. Ou, H. Xiao, X. Guan, B. Han, Nanomaterials-enabled multifunctional concrete and structures, in: Nanotech. Civil Infra, Springer, 2011, pp. 131–173.
[36] A. Al-Dahawi, G. Yıldırım, O. Öztürk, M. Şahmaran, Assessment of self-sensing capability of Engineered Cementitious Composites within the elastic and plastic ranges of cyclic flexural loading, Constr. Build. Mater. 145 (2017) 1–10.
[37] T.C. Hou, Wireless and Electromechanical Approaches for Strain Sensing and Crack Detection in FRC Materials PhD Dissertation, Civil and Environmental Engineering, University of Michigan, Ann Arbor, MI, 2008.
[38] S. Yeşilmen, Y. Al-Najjar, M.H. Balav, M. Şahmaran, G. Yıldırım, M. Lachemi, Nano-modification to improve the ductility of cementitious composites, Cem. Concr. Res. 76 (2015) 170–179.
[39] G. Yıldırım, B. Dündar, B. Alam, İ.Ö. Yaman, M. Şahmaran, Role of nanosilica on the early-age performance of natural pozzolan-based blended cement, ACI Mater. J. 115 (6) (2018) 969–980.
[40] G. Land, D. Stephan, The influence of nano-silica on the hydration of ordinary Portland cement, J. Mater. Sci. 47 (2) (2012) 1011–1017.
[41] T. Manzur, N. Yazdani, M. Emon, A. Bashar, Effect of carbon nanotube size on compressive strengths of nanotube reinforced cementitious composites, J. Mater. 2014 (2014).
[42] H. Siad, M. Lachemi, M. Şahmaran, H.A. Mesbah, K.A. Hossain, Advanced Engineered Cementitious Composites with combined self-sensing and self-healing functionalities, Constr. Build. Mater. 176 (2018) 313–322.
[43] S.P. Shah, M.S. Konsta-Gdoutos, Z.S. Metaxa, P. Mondal, Nanoscale modification of cementitious materials, Nanotech. Constr. 3 (2009) 125–130.
[44] L. Zongjin, Advanced Concrete Technology, John Wiley & Sons, Inc., Hoboken, New Jersey, 2011.
[45] F. Reza, G.B. Batson, J.A. Yamamuro, J.S. Lee, Resistance changes during compression of carbon fiber cement composites, J. Mater. Civil Eng. 15 (5) (2003) 476–483.
[46] F.J. Baeza, E. Zornoza, L.G. Andión, S. Ivorra, P. Garcés, Variables affecting strain sensing function in cementitious composites with carbon fibers, Comput. Concr. 8 (2011) 229–241.
[47] S. Wang, V.C. Li, Engineered Cementitious Composites with high-volume fly ash, ACI Mater. J. 104 (3) (2007) 233–241.
[48] Q.S. Banyhussan, G. Yıldırım, E. Bayraktar, S. Demirhan, M. Şahmaran, Deflection-hardening hybrid fiber reinforced concrete: the effect of aggregate content, Constr. Build. Mater. 125 (2016) 41–52.
[49] Q.S. Banyhussan, G. Yıldırım, Ö. Anıl, R.T. Erdem, A. Ashour, M. Şahmaran, Impact resistance of deflection-hardening fiber reinforced concretes with different mixture parameters, Struct. Concr. 20 (3) (2019) 1036–1050.
[50] S. Demirhan, G. Yıldırım, Q.S. Banyhussan, K. Koca, Ö. Anıl, R.T. Erdem, M. Şahmaran, Impact behaviour of nano-modified deflection-hardening fibre reinforced concretes, Mag. Concr. Res. (2019) 1–46.
[51] M.H. Sarwary, G. Yıldırım, A. Al-Dahawi, Ö. Anıl, K.A. Khiavi, K. Toklu, M. Şahmaran, Self-sensing of flexural damage in large-scale steel-reinforced mortar beams, ACI Mater. J. 166 (4) (2019).
[52] H.W. Whittington, J. McCarter, M.C. Forde, The conduction of electricity through concrete, Mag. of Concr. Res. 33 (114) (1981) 48–60.
[53] P. Mehta, P. Monterio, Concrete: Microstructure, Properties and Materials, 3rd ed., McGraw-Hill, USA, 2006.
[54] C.S. Smith, Piezoresistance effect in germanium and silicon, Phys. Rev. 94 (1) (1956) 42–49.
[55] D. Wang, S. Wang, D.D.L. Chung, J.H. Chung, Comparison of the electrical resistance and potential techniques for the self-sensing of damage in carbon fiber polymer-matrix composites, J. Intel. Mat. Syst. Str. 17 (2006) 853–861.